

CHARACTERIZATION OF A STRONG SWIRLING FLOW WITH PRECESSING VORTEX CORE BASED ON MEASUREMENTS OF VELOCITY AND LOCAL PRESSURE FLUCTUATIONS

P.M. Anacleto¹, E.C. Fernandes¹, M.V. Heitor¹ and S.I. Shtork^{1,2}

¹ Laboratory of Thermofluids, Combustion and Energy Systems
Center for Innovation, Technology and Policy Research, IN+
Instituto Superior Técnico, Technical University of Lisbon
Av. Rovisco Pais, 1049-001 Lisbon, Portugal
<http://in3.dem.ist.utl.pt/>

² Institute of Thermophysics, Siberian Branch of Russian Academy of Sciences
Lavrentyev Ave. 1, 630090 Novosibirsk, Russia
<http://www.itp.nsc.ru>

ABSTRACT

The swirling flow in a model lean premixed combustor is studied for flow conditions characterized by the presence of a breakdown zone and flow pulsations caused by hydrodynamic instabilities in the form of a precessing vortex core. The precessing frequency and the swirl level of the flow are used to characterize typical flow regimes that may lead to low NO_x emissions and high fuel efficiencies in practical combustors. This is shown to be associated with stable recirculation zones defined according to characteristic maps for frequency and pressure drop measurements for non-reacting conditions. Accordingly, LDA measurements (see figure 1) illustrated the presence of developed breakdown region in a primary zone of the combustor with high turbulence level, at optimal regime, that provides the necessary condition for turbulent stabilization process.

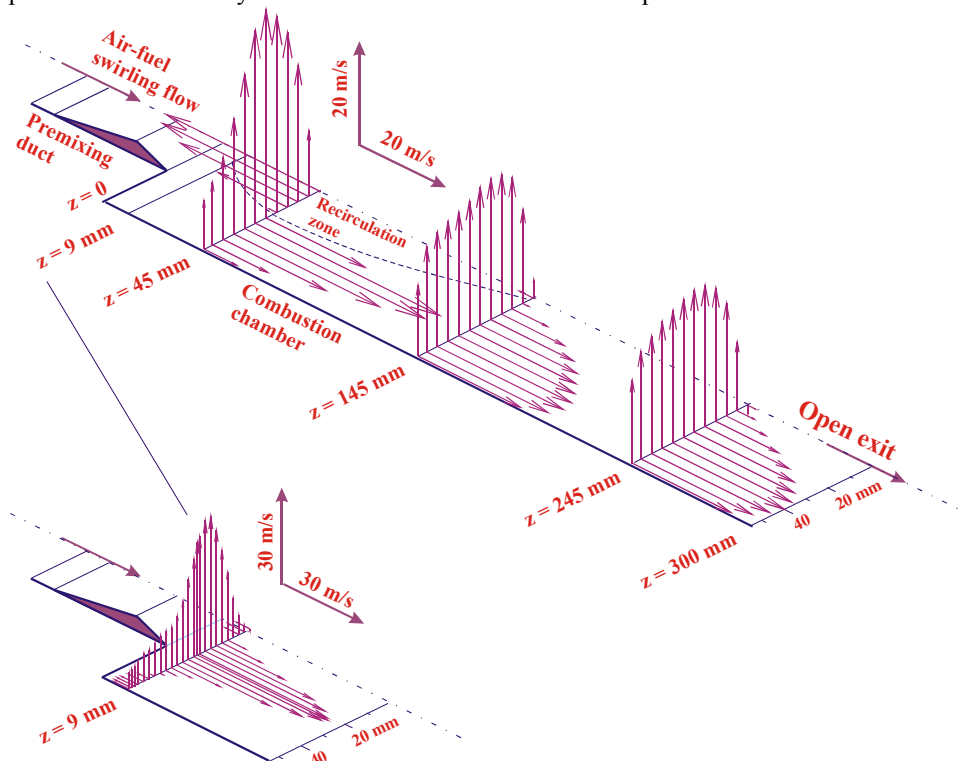


Figure 1. Axial and tangential mean velocity components of the flow in the combustion chamber operating at optimal configuration with liquid Jet-A fuel burning. Air mass flow rate $Q_m = 0.046$ kg/s, $S = 1.05$, $\Phi = 0.5$, $T_{air} = 300^\circ\text{C}$.

1. INTRODUCTION

In the context of low emissions combustors, as defined by Bahr (1995), the recent work of Anacleto and Heitor (2001) in a *Lean Premixed Prevaporized*, LPP, model combustor provides evidence of very low NO_x emissions at high fuel efficiencies by means of a central recirculation zone formed due to breakdown of a highly-swirled jet. The reverse flow playing a critical role in flame holding is associated with flow pulsations in the form of a precessing vortex core, PVC, as discussed by Chanaud (1965), Cassidy & Falvey (1970), Gupta et al. (1984), Dellenback et al. (1988), Yazdabady et al. (1994), Fick et al. (1997), and Guo et al. (2001), among others. This has motivated the present work, mainly because the effect of a PVC on combustion performance has been shown to depend on several factors, such as the fuel supply and mixture ratio (Syred & Beer, 1973; Bertrand & Michelfelder, 1976; Gupta et al., 1984; Froud et al., 1995; Coats, 1996), thus affecting overall combustion performance in practical combustors.

It should also be noted the increasing regulation for NO_x emissions is promoting the design of combustors to be operated with lean premixed flames, which are particularly prone to combustion instabilities (e.g. Culick, Heitor and Whitelaw, 1995; Lieuwen et al., 2001), apart from being associated with a vortex core that is formed as a kind of a hydrodynamical flow instability. The resulting large amplitude velocity and pressure pulsations cause undesirable factors, such as loud noise and vibrations, which in turn may be amplified and coupled with the natural acoustics modes of the combustor. On the other hand, fluid precessing motion may help to reduce NO_x emissions and fuel consumption through enhanced large-scale turbulence, as shown for the precessing jet burners of Schneider et al. (1997), Megalos et al. (2001).

Since the analysis shows that the precessing structure may play a significant role in combustion processes typical of practical combustors, the work reported in this paper is aimed to study critical PVC parameters in a model combustor that may characterize swirl flow regimes and improve combustor performance (Sivasegaram & Whitelaw, 1991; Paschereit et al., 1999). In our approach the combustor performance is considered in terms of fuel efficiency and pollutants emission, as calculated from major species levels at the combustor exit (Yegian & Cheng, 1998). The experiments are reported for atmospheric pressure to allow considering the detailed effect of various geometrical and physical parameters, although this does not avoid checking at more expensive elevated pressures (Shaffar & Samuelsen, 1998).

For example, an important part of our studies is based on isothermal experiments making use of one-point acoustic measurements to characterize the precessing flow and static pressure drops to characterize the intensity of flow swirling. We use these parameters to discuss the conditions for optimal combustor performance through the analysis of stability maps to effectively identify flow aerodynamic structure that was verified also by direct LDA measurements. The results are encouraging for low cost design of future low-NO_x aero and stationary gas turbine combustors.

2. EXPERIMENTAL METHOD

The experimental configuration consists of a single fuel injector positioned in the center line of a cylindrical prevaporising duct, with flame stabilization provided through a sudden expansion at the combustor entrance (Figure 1). The premixing chamber is a cylindrical duct with an inner diameter of $d=50\text{mm}$ and a length of 166mm. Gaseous fuel (propane) was supplied before premixing duct (Figure 1) and liquid (Jet-A1) fuel was introduced through commercial nozzles with different spray angles as documented by Anacleto & Heitor (2001). The combustor itself is made of cylindrical stainless-steel ducts with an inner diameter of $D=110\text{mm}$ and a total length of 300mm. The various combustor modules include sections that provide the necessary optical access to the flow, to allow the use of laser techniques to visualize and quantify the inner flow, as also described in detail by Anacleto & Heitor (2001).

The experiments were conducted at atmospheric pressure. A purpose-built pre-heater delivers non-vitiated air up to $T_0=500^\circ\text{C}$, and a maximum air mass flow rate up to 0.1kg/s. The swirl generator has a variable geometry, which allows shifting the angle of the vanes between 0° and 60° , in order to control the swirl level of the flow. The flow rate was defined through the pressure drop on a standard diaphragm, as measured with U-type water manometers. The swirl number was defined through the swirler geometry according to Gupta et al. (1984).

Quantitative flow visualization was performed using a high-speed CCD camera (*Kodak Motion Corder Analyzer*), allowing flow patterns recording with a sampling rate up to 10000 images per second. Standard aluminum particles and smoke produced by a smoke generator were used as flow markers, while

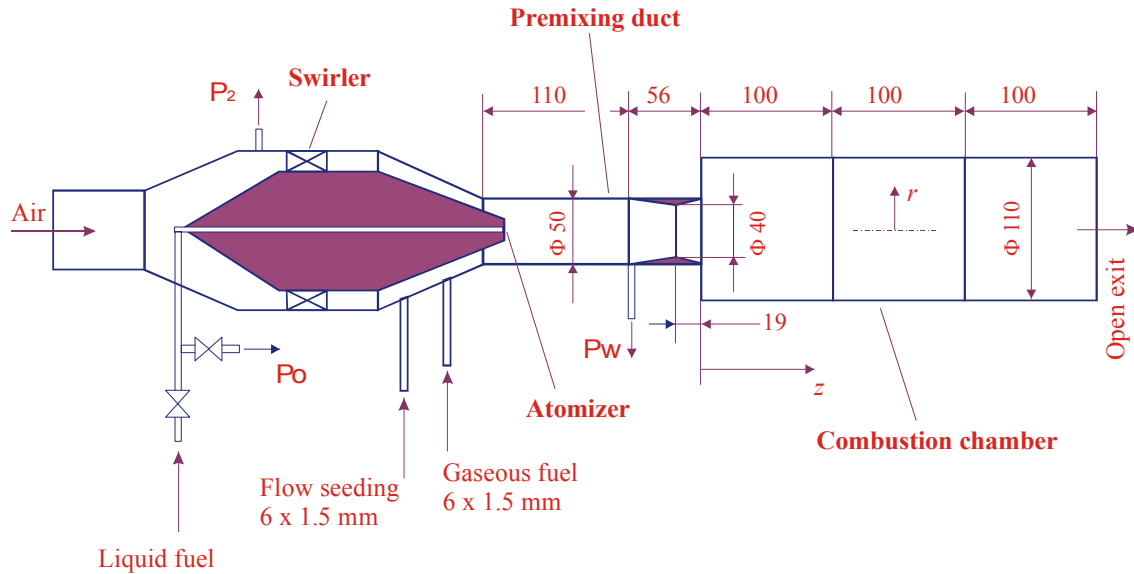


Figure 2. Details of the experimental set-up.

the flow was illuminated with a 2mm laser light sheet, originated from a 2W Argon-Ion laser beam making use of a cylindrical lens beam expander.

Velocity was measured by a dual-beam, forward-scatter mode laser Doppler velocimeter based on a 2 W Argon-Ion laser. Aluminum particles were used for flow seeding in reacting conditions and paraffin oil droplets produced by a standard jet atomizer were utilized for isothermal flow measurements. Sensitivity to the flow direction was provided by light-frequency shifting from acousto-optic modulation at 10 MHz. The output signal of the laser velocimeter was processed by a frequency counter (TSI 1980-B), as described in detail by Anacleto & Heitor (2001). Major gas species were quantified making use of a standard species analyzer system (Anacleto & Heitor, 2001).

The instantaneous pressure field was identified making use of a noise measuring system based on a condenser microphone (B&K-2230) and semi-infinite probe with the tip installed at the premixing chamber exit (Figure 4). The microphone signal was acquired by a Fulcrum DT3808 board installed into a PC, where frequency analysis was processed with an accuracy of ± 1.22 Hz.

The vortex flow regime generated in the present configuration is characterized by integral parameters, which include the averaged frequency of PVC precession and the static pressure difference across the vortex flow, $\Delta P_1 = P_w - P_0$ (where P_0 is the pressure at the vortex axis, as taken from the atomizer hole, and P_w is the pressure on the wall, as taken before the nozzle upstream of the combustor chamber). This pressure drop quantifies the *vortex intensity* (Alekseenko et al., 1999) and was measured in the absence of fluid through the fuel injector. Besides, total static pressure drop over the vortex experimental model $\Delta P_2 = P_2 - P_{atm}$ (where P_2 is the pressure at the swirling device wall before blades and P_{atm} is the atmospheric pressure) was measured and amplitude of harmonic corresponding to PVC frequency in acoustic signal was defined. The Reynolds number of the flows analyzed, as based on the mean axial velocity at the inlet section of the combustor, is about 10^5 . In addition, the diameter and averaged velocity at the premixing duct exit (with a diameter $d_0=40$ mm) were used to calculate the Strouhal number, $Sh = f d_0 / U_0$, and the differential pressure $\Delta P^* = 2 \Delta P / \rho U_0^2$.

3. RESULTS AND DISCUSSION

3.1. Swirl number evaluation

Figure 3 presents the swirl number calculated by integration of measured velocity profiles inside the swirl flow near the nozzle outlet ($z = 10$ mm) at different angles ϕ :

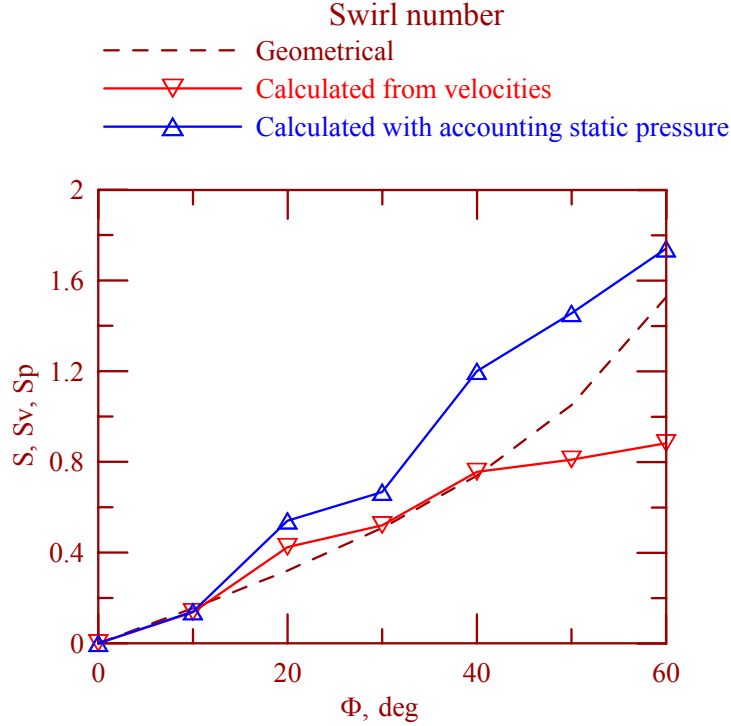


Figure 3. Comparison of the geometric swirl number S with those calculated through integration of measured velocity profiles in the primary zone of combustor (with and without account for static pressure distribution, S_v and S_p consequently).

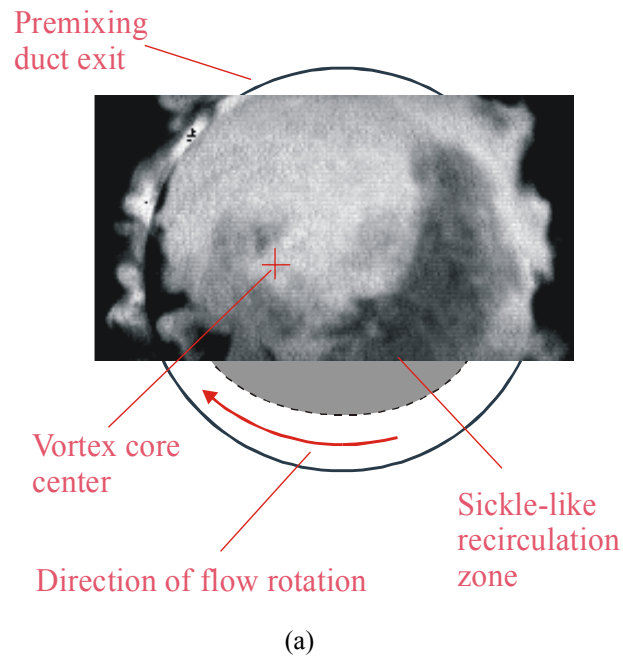
$$S_v = \frac{\int_0^{\infty} \rho u w r^2 dr}{R \int_0^{\infty} \rho u^2 r dr}, \quad (4)$$

where the characteristic radius is taken as $R = d_0 / 2$. Comparison of those values with data calculated through geometric characteristic of swirler device (Gupta et al., 1984) demonstrates a fair agreement up to the angle of 40° . The difference at higher swirl numbers can be explained by contribution of static pressure in the axial moment. Taking into account the static pressure according to Milosavljevic, et al. (1990) gives us the values above the geometric parameter; although it is obvious there is no a complete balance between centrifugal forces and radial gradient of static pressure (in this cross-section the flow expands, Figure 4). So, in our paper we use geometrical swirl number, which gives expected values between these two limiting cases.

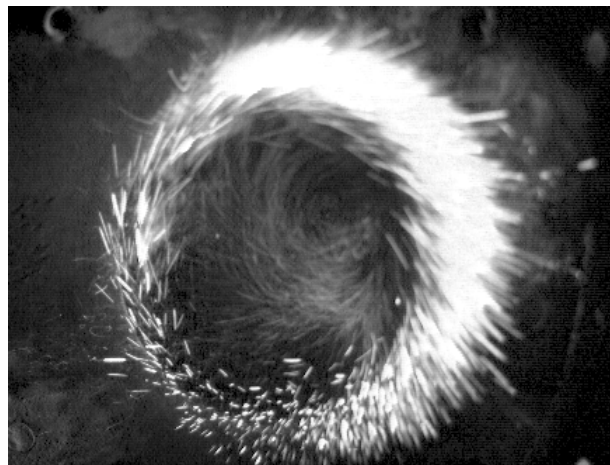
3.2. Instantaneous flow structure

Flow visualization with high-speed video recording demonstrated that at the exit of premixing chamber a zone of reverse flow is formed with a strong PVC at its boundary. The off-center vortex core could be seen in a cross-section, normal to the longitudinal axis of the chamber at visualization by aluminum particles (Figure 4b). The vortex core position for smoke picture (Figure 4a) was defined and reconstructed from a video movie of the whole circle of flow precession. The sickle-like or crescent dark region within the jet region corresponds to an area of reverse flow (as confirmed by analyzing video records of the flow pattern along a horizontal cross section), which contains ambient air free of smoke. On the other hand, the vortex core transports smoke and is attached to one of the tips of the crescent dark region, moving before it.

The analysis clearly suggests that the instantaneous flow structure associated with PVC is more complex than has been presented in the literature in the form of time averaged velocity profiles (e.g.,



(a)



(b)

Figure 4. Sample images of flow pattern with the PVC forming near the exit of the premixing duct for $S = 1.26$, $T_{air} = 20^\circ C$ (rotation in clockwise direction). Visualization by smoke at $Re = 15000$ (a) and aluminium particles at $Re = 19000$ (b) in plane across of the vortex axis at $z = 27\text{ mm}$.

Gupta, Lilley and Syred, 1984). In fact, our qualitative results agree with those of Yazdabadi et al. (1994) using phase-averaged measurements in a cross section of a cyclone separator exit, which also indicate an attached reverse zone to the PVC center. Their results indicate also a lagging rotating reverse flow area in the manner we observe. Another their conclusion consists in that zones of highest tangential and forward axial velocities are also attached to the PVC and rotating together with it. All these facts lead to complex spatial flow characteristics in the presence of a precessing vortex core.

Our sample results on averaged and instantaneous flow field characteristics near the exit of the premixing chamber confirm the mentioned details of PVC induced flow (Figure 5). The averaged velocity component vectors present usual features of strongly swirling flow in a form of annulus conical jet embracing the zone of recirculating motion. Time series of LDA signals show presence of intensive pulsations of all velocity components. Traces of tangential and axial velocity components follow near a sine form at $r=0$ for tangential velocity and $r=10\text{ mm}$ for axial component. This is because of at the center

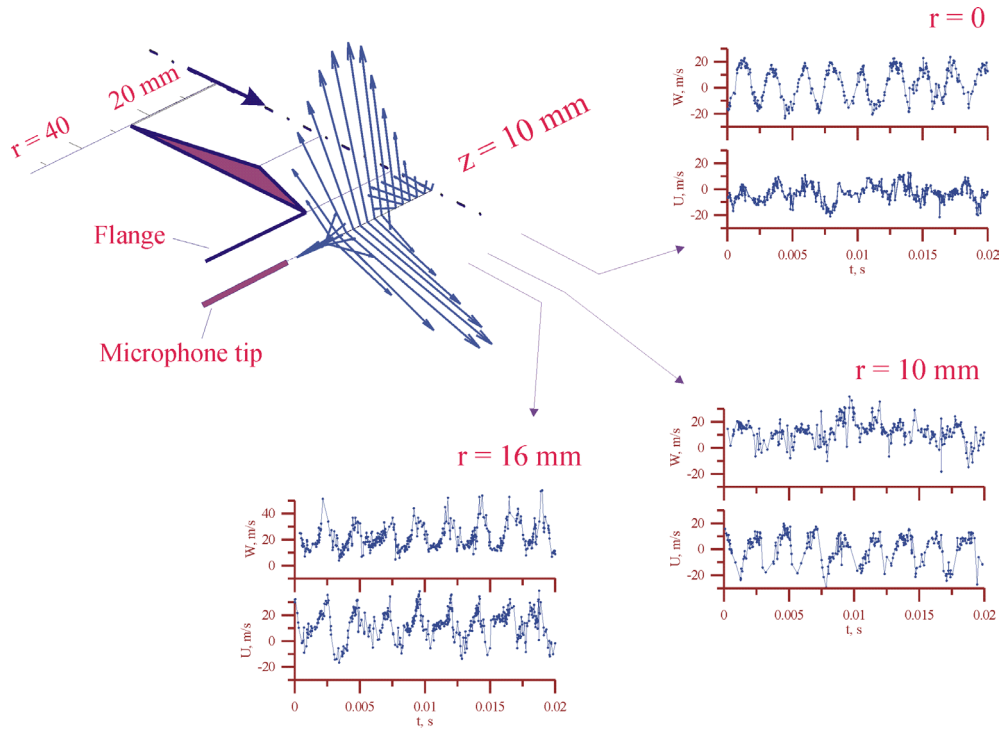


Figure 5. Projections of 3D velocity vector and time series for LDA signal in the PVC formation zone (experiments without combustion chamber at $z = 10$ mm, $S = 1.05$, $Re = 8.1 \cdot 10^4$).

PVC induces the rotational velocities of different signs (with zero mean value) and from the other hand at boundary of reverse flow zone ($r=10$ mm), which could be identified as approximate position of the PVC center (Gupta et al., 1984), the rotating reverse zone alternates with a forward flow giving as result zero mean axial velocity. Let us note that namely at $r=10$ mm occurs an absolute maximum of the backward flow intensity indicating off-center rotating reverse flow zone. Local maxima of fluctuating tangential and forward axial velocities take place at radius $r=16$ mm with a phase angle corresponding to angular position of PVC center (as it follows from the data of Yazdabadi et al., 1994).

3.3. Swirling flow integral parameters

It is accepted that the swirl number is the key parameter for structure of swirl flow in a vortex chamber that allows to provide effective control over working processes (Hoekstra et al., 1999; Zhou et al., 2000). In this context the Figure 6 presents analysis of the integral characteristics of swirling flow at changing the blade angle. If taken in dimensionless form these characteristics indicate three different stages of vortex core and swirl jet development, as the swirl degree increases. In region I, for swirl levels below $S=0.5$, rotation of the vortex core grows sharply with S , corresponding to a sharp increase in the radial pressure difference (Figure 6b). The jump like vortex intensification is limited by vortex breakdown at $S=0.5$ and results in a PVC with discrete peaks in the pressure and velocity spectra. Further increase of the swirl number is compensated by the related spreading of the recirculation zone and expansion of vortex core, resulting in region II, which is characterized by constant radial pressure differences (namely for large Re). The precession frequency in this region decreases with S up to a minimum value due to growth of PVC rotation radius (Figure 6a). After full development of the recirculation zone, PVC rotation frequency starts to increase in region III as it has been noted in previous experiments (Cassidy & Falvey, 1970). Amplitude of dominant harmonic in this region takes much more large values than previously and considerably grows with swirl number (Figure 6c), because of the more stable and regular precession produces more narrow and high pick in pressure fluctuation spectra. Looking at the dependence for pressure drop over the vortex chamber we can notice that before appearance of reverse flow there is no any noticeable the input pressure loss (Figure 6d); only after the swirl number becomes more than 0.51 pressure drop starts to increase due to energy dissipation in a high turbulent recirculation zone.

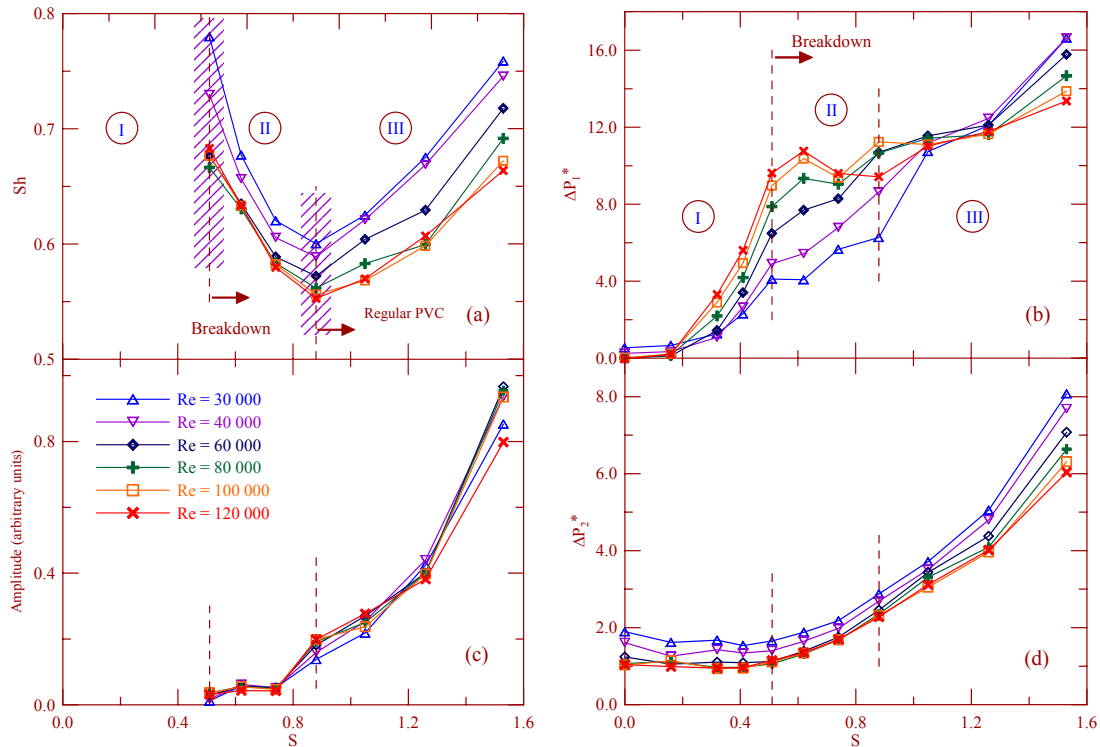


Figure 6. The dimensionless integral parameters of the flow as function of swirl number S and Reynolds number Re :

- (a) Frequency of dominant harmonic in pressure signal spectra;
- (b) Radial difference of static pressure in premixing chamber;
- (c) Amplitude of dominant harmonic (arbitrary units);
- (d) Overall static pressure drop.

3.4. Averaged flow structure characterization

To understand causes of unusual behavior of swirling flow at changing the swirl number the detailed measurements of local velocities for different swirler blade angles have been done. The parameters of averaged flow taken from the measured profiles of velocity inside the swirl flow are shown in Figure 7. We see that the radii for the maximal axial and tangential velocities increase drastically with the swirl number. This is an indication of abrupt radial expansion of the jet that causes also the axial velocity deceleration on the axis. The zone of rapid radial expansion (and decreasing of the centerline axial velocity) corresponds to the zone I in Figure 6. Then, for zone II at $S > 0.5$, with appearance of negative velocities along axis we observe generation of PVC, which is registered as expressed picks in spectra of pressure pulsations. One can see from the graph in Figure 7a that flow in zone II keeps expanding with an increasing of the swirl number: this means increasing of the PVC rotation radius for bringing the mentioned anomalous the precessing frequency drop. LDA-measurements indicate that at $S > 0.74$ we step in the zone III with a fully developed flow structure (the positions of maxima are stable, as well as the intensity of reverse flow). In addition, Figure 8 demonstrates change in the dimensionless circulation of the mean flow, which is a linear dependence on the geometrical swirl number; this also confirms that this parameter is the correct choice for description of a swirl flow.

3.5. Reacting flow tests

Next studies were done to evaluate influence of swirl number and accordingly flow structure on combustor performance. Figure 9a presents the range of combustor operation defined by the flammability and flashback limits and shows that for increasing swirl intensity, the operation range is reduced to a narrow interval of equivalence ratios, but this does not affect the target regime of “ultra-lean” conditions

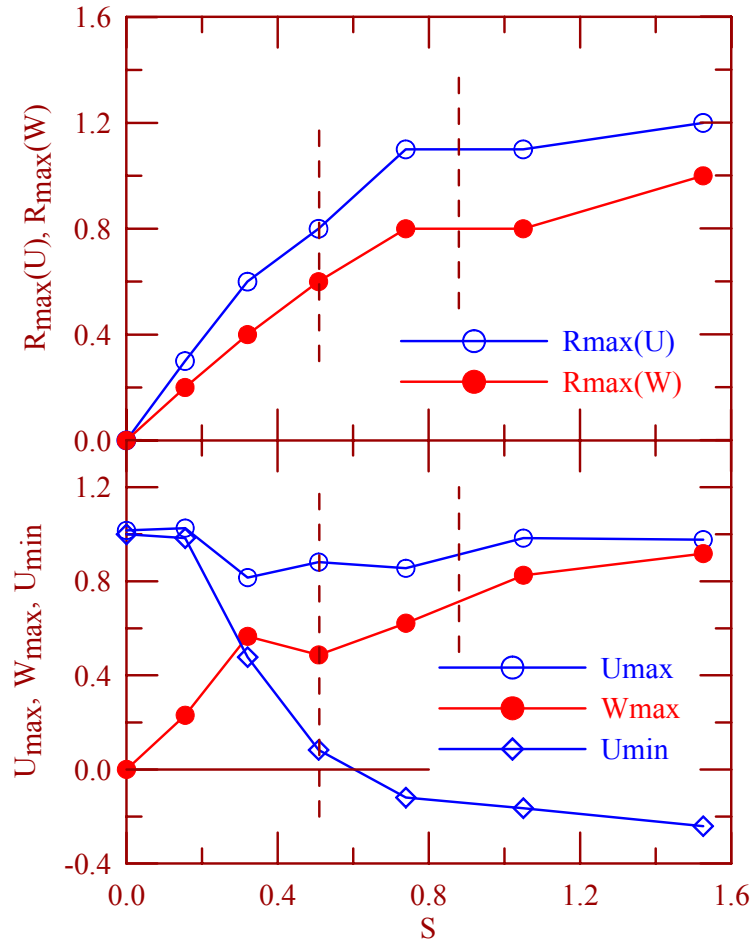


Figure 7. Characteristics of averaged flow in the combustor primary zone as function of swirl number:
 (a) Dimensionless radii for positions of the maximums of velocity components (scaled by $d_0/2$);
 (b) Dimensionless maximal values in the profiles of velocity components together with center line axial velocity U_{min} (scaled through U_0)

away from the flashback. The results presented in Figure 9b confirm that increasing swirl intensity leads to a considerable reduction of NO_x and CO at exit of the combustion chamber that depends on the complete liquid fuel vaporization in the premixing duct and stable recirculating flow zone (see Figure 6). Based on results obtained for isothermal (Figure 6) and reacting conditions (Figure 9) an optimal working condition is defined for $S = 1.05$, above 0.88, but below 1.26 (flashback limit). This working condition is characterized by a stable aerodynamics, good combustion performance and similar pollutant concentration (NO_x and CO) for gaseous and jet fuel operation mode. Detailed measurements of flow characteristics for the optimal regime are presented in Figure 1, which confirms presence of developed breakdown region providing combustion stabilization.

4. CONCLUSIONS

The work presents new data relating the existence of a breakdown zone and flow pulsations caused by hydrodynamic instabilities in the form of a *precessing vortex core* with the downstream combusting flow in a model combustor. The results are of interest to practical combustors in that flow regimes that may lead to low NO_x emissions are prone to increased flow oscillations. In fact, considering the design of combustors to be operated with lean premixed flames, it is evident that the target would be a regime with a steady recirculation zone and stabilized combustion. According to the stability maps of

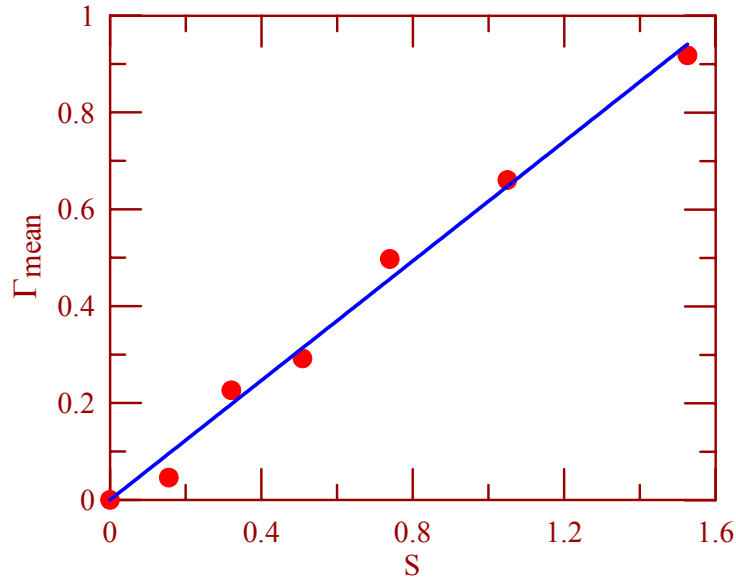


Figure 8. Dimensionless circulation $\Gamma_{mean} = \frac{R_{max}(W) \times W_{max}}{\frac{d_0}{2} \times U_0}$ of averaged flow.

Figure 6, this would occur for our geometry for $S > 0.88$, where the flow exhibits stable parameters at varying both flow rate and swirl number. The results of Fig. 3, for $S = 1.05$, confirm this expectation, with complete fuel vaporization upstream of the combustion zone, local lean conditions in combustion chamber and low NOx emissions at the combustor exit. Flame stabilization occurs due to swirling jet breakdown and provides complete fuel burning at low equivalent ratios and, accordingly, relatively low gas temperatures (Bahr, 1995).

In general, the practical significance of the work is based on the evidence shown between the vortex flow integral parameters, which might be acquired by relatively simple techniques, and combustor performance. The effect shown of the frequency of PVC rotation and of the total radial pressure difference in the premixing chamber on vortex flow development downstream of swirl jet breakdown is important to predict combustor regimes. Consequently, optimal LPP combustor design should be associated with swirling flow regimes with developed and stable recirculation zones defined according to characteristic maps for frequency and pressure depression on vortex axis. Accordingly, LDA measurements illustrated the presence of developed breakdown region in a primary zone of the combustor with high turbulence level, at optimal regime, that provides the necessary condition for turbulent stabilization process.

ACKNOWLEDGEMENTS

The authors are pleased to acknowledge support from the Portuguese Science and Technology Foundation (Grant N PCT/1999/EME/34768). Sergei I. Shtork is a post-doctoral research fellow at the IST's Laboratory of Thermofluids, Combustion and Energy Systems under the Fellowship SFRH/BPD/1641/2000.

REFERENCES

1. Alekseenko S.V., Kuibin P.A., Okulov V.L., Shtork S.I. (1999), "Helical vortices in swirl flow", *J. Fluid Mech.*, **382**, pp. 195-243.
2. Anacleto P.M. and Heitor M.V. (2001), "On the performance of lean-premixed combustion", submitted for publication in *Experiments in Fluids*.

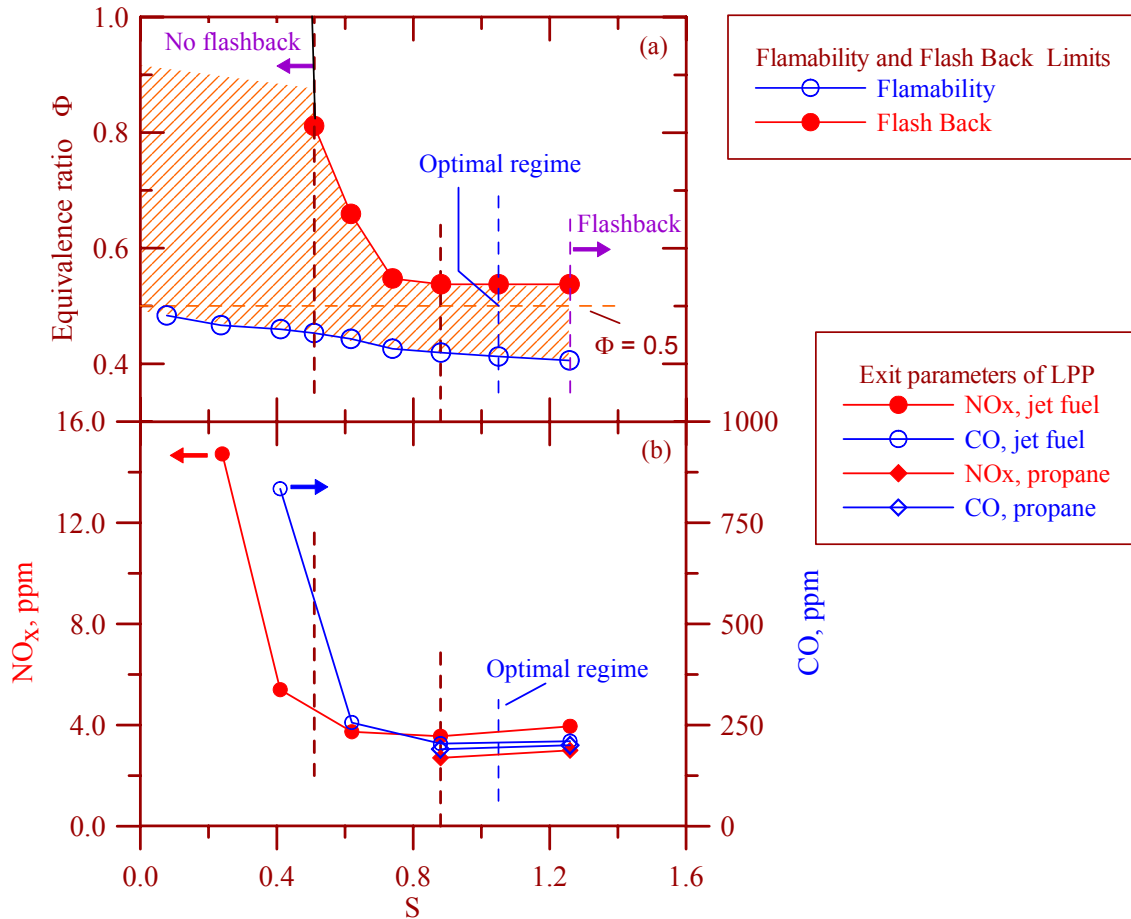


Figure 9. Combustor characteristics as function of swirl number:

(a) Flammability and flashback limits;

(b) Averaged over exit cross section NO_x and CO levels (hollow and filled symbols) at burning propane and jet fuel (rhombus and circles) with $\Phi = 0.5$. Air mass flow rate $\dot{Q}_m = 0.046$ kg/s, $T_{air} = 300^\circ\text{C}$.

3. Bahr D. (1995), "Aircraft turbine engine NO_x emissions abatement", in "Unsteady Combustion", Eds. F. Culick, M. Heitor and J. Whitlaw, Kluwer Academic Publ., NATO ASI Series, Vol. E 306, pp. 234-264.
4. Bertrand C., Michelfelder S. (1976), "Experimental investigation of noise generated by large turbulent diffusion flames", Sixteenth Symp. (Intl.) on Combust. The Combustion Institute, pp. 1757-1769.
5. Cassidy J.J., Falvey, H.T. (1970), "Observation of unsteady flow arising after vortex breakdown", *J. Fluid Mech.*, 41, pp. 727-736.
6. Chanaud R. C. (1965), "Observations of oscillatory motion in certain swirling flows", *J. Fluid Mech.*, 21(1), pp. 111-127.
7. Coats C.M. (1996), "Coherent structures in combustion", *Prog. Energy Combust. Sci.*, 22, pp. 427-509.
8. Dellenback P.A., Metzger D.E. and Neitzel G.P. (1988), "Measurements in turbulent swirling flow through an abrupt axisymmetric expansion", *AIAA Journal*, 26(6), pp. 669-681.
9. Escudier M., (1988), "Vortex breakdown: observations and explanations", *Prog. Aerospace Sci.*, 25, pp. 189 - 229.
10. Fick W., Griffiths A. J. and O'Doherty T. (1997), "Visualization of the precessing vortex core in an unconfined swirling flow", *Optical Diagnostics in Engineering*, 2(1), pp. 19-31.

11. Froud D., O'Doherty T. and Syred N. (1995), "Phase averaging of the precessing vortex core in a swirl burner under piloted and premixed combustion conditions", *Comb. & Flame*, 100, pp. 407-412.
12. Heitor M.V., Moreira A.L.N. (1992), "Velocity characteristics of a swirling recirculating flow", *Exp. Thermal. Fluid Sci.*, 5(3), pp. 369-380.
13. Heitor M.V., Whitelaw J.H. (1986), "Velocity, temperature, and species characteristics of the flow in a gas-turbine combustor", *Comb. & Flame*, 64, pp. 1-32.
14. Hoekstra A.J., Derksen J.J. and Van Den Akker H.E.A. (1999), "An experimental and numerical study of turbulent swirling flow in gas cyclones", *Chemical Engineering Science*, 54 (13-14), pp. 2055-2065.
15. Guo B., Langrish T.A.G., Fletcher D.F. (2001), "Simulation of turbulent swirl flow in an axisymmetric sudden expansion", *AIAA Journal*, 39(1), pp. 96-102.
16. Gupta A.K., Lilley D.G., Syred N. (1984), "*Swirl Flows*", Abacus Press.
17. Lieuwen T., Torres H., Johnson C., Zinn B.T. (2001), "A mechanism of combustion instability in lean premixed gas turbine combustors", *J. of Engng. Gas Turbine and Power*, 123, pp. 182-189.
18. Megalos N.P., Smith N.L., Zhang D.K. (2001), "The potential for low NO_x from a precessing jet burner of coal", *Comb. & Flame*, 124, pp. 50-64.
19. Milosavljevic V.D., Taylor A.M.K.P., Whitelaw J.H. (1990), "Influence of burner geometry and flow rates on the stability and symmetry of swirl-stabilized nonpremixed flames", *Comb. & Flame*, 80, pp. 196-208.
20. Paschereit C.O., Gutmark E., Weisenstein W. (1999), "Coherent structures in swirling flows and their role in acoustic combustion control", *Phys. of Fluids*, 11(9), pp. 2667-2678.
21. Shaffar S.W., Samuelsen G.S. (1998), "A liquid fueled, lean burn, gas turbine combustor injector", *Combust. Sci. & Technology*, 139, pp. 41-57.
22. Sivasegaram S., Whitelaw J.H. (1991), "The influence of swirl on oscillations in ducted premixed flames", *Combust. Sci. & Technology*, 85, pp.195-207.
23. Schneider G.M., Froud D., Syred N., Nathan G.J. and Luxton R.E. (1997), "Velocity measurements in a precessing jet flow using a three dimensional LDA system", *Experiments in Fluids*, 23, pp. 89-98.
24. Yazdabady P.A., Griffiths A.J. & Syred N. (1994), "Characterization of the PVC phenomena in the exhaust of cyclone dust separator", *Experiments in Fluids*, 17, pp. 84-95.
25. Yegian D. T., Cheng R. K. (1998), "Development of a Lean Premixed Low-swirl Burner for Low No_x Practical Applications", *Combust. Sci. & Technology*, 139, pp. 207-227.
26. Zhou L.X., Li Y., Chen T. and Xu Y. (2000), "Studies on the effect of swirl numbers on strongly swirling turbulent gas-particle flows using a phase-Doppler particle anemometer", *Powder Technology* 112:(1-2), pp. 79-86.